A Novel EMI Filter Design Method for Switching Power Supplies

Sheng Ye, *Student Member, IEEE*, Wilson Eberle, *Student Member, IEEE*, and Yan-Fei Liu, *Senior Member, IEEE*

***Abstract*—This paper introduces an improved and simplified method to design electromagnetic interference (EMI) filters for both dc–dc and ac–dc switching power supplies. This method uses the practical approach of measuring the power supply noise spectrum and using the data to calculate the maximum possible magnitude and minimum possible magnitude of the differential mode and common mode noise impedances. The noise impedance magnitude information aids the design of the EMI filter. Phase information for the noise impedance is not required. In addition, information about the topology and control method of the power supply is not needed. This method solves the limitations of existing EMI filter design methods, which are either too complicated to use, or are based on ideal cases that neglect the noise impedance. The analysis and experimental results show that this method can guarantee that the required attenuation can be achieved, especially at low frequencies.**

***Index Terms*—Electromagnetic interference (EMI), EMI filter, noise impedance.**

I. INTRODUCTION

IN COMMUNICATION systems, distributed power systems are widely used. In these systems, "off the shelf" power modules are used to convert the input voltage to a lower voltage to power digital and/or optical circuits. However, these power modules normally cannot meet the FCC, or CISPR electromagnetic interference (EMI) regulatory standards for conducted EMI. As a result, additional EMI filters, normally both common mode (CM) and differential mode (DM), are needed at the input of these power modules in order to filter out the switching noise and eliminate electromagnetic interference to other equipment.

The design of EMI filters is not trivial for two reasons: 1) the system engineers, or board engineers, do not know the details of the power module circuits and 2) EMI filter design is considered a "black art" because little is known about the EMI source. In addition, interaction between the EMI source impedance and the EMI filter's output impedance can cause poor noise attenuation. Therefore, a simple and effective EMI filter design method is required.

Unfortunately, only limited research has been done on the methods of designing EMI filters to meet system requirements. Trial and error methods are often used in EMI filter design. Furthermore, existing EMI filter design methods usually ignore the noise impedance of the switching power supply (SPS), which results in either over design, or the system requirements not being met.

Existing EMI filter design methods are reviewed in Section II of this paper. The effect of the noise impedance on EMI filter design, and the noise attenuation performance of the EMI filter are analyzed in Section III. In Section IV, a procedure is presented to determine the maximum possible value and minimum possible value of the CM and DM noise source impedances. A new method to design EMI filters, utilizing the maximum and the minimum noise source impedance, is proposed in Section V. The proposed method is easy to implement and does not require the phase information of the noise source impedance. Experimental results are presented in Sections V and VI to illustrate that the proposed method is a simple and effective way to design EMI filters for both dc–dc and ac–dc switching power supplies. Section VII is the conclusion.

II. REVIEW OF EXISTING EMI FILTER DESIGN METHODS

A procedure to design EMI filters was introduced in [1]. However, the impact of the noise impedance of the power supply was not considered, so this procedure cannot guarantee that the required attenuation can be achieved. In addition, several design iterations may be needed.

In [2], a method was introduced to measure the DM and CM noise impedances. Three assumptions were made: 1) the CM noise impedance was much greater than the equivalent line impedance stabilization network (LISN) resistance, 25 Ω, 2) the large capacitor and inductor always behaved ideally, and 3) expensive equipment (e.g., an impedance analyzer with a high degree of accuracy at low impedances ($<10\ \Omega$) was available to measure very small impedances. Unfortunately, these assumptions are not always valid in the actual case. When these assumptions are not valid, it is impossible for us to know the noise impedance accurately by using the method in [2]. Even when the assumptions are valid, the method is very complex. Specifically, the method used to measure the noise impedance's phase angle is complicated.

Due to the limitations of the existing EMI filter design methods, a simple and accurate EMI filter design method is needed. In this paper, a new, simple, and accurate EMI filter design method is proposed.

III. NOISE IMPEDANCE'S EFFECT ON THE EMI FILTER

The noise impedance is due to circuit parameters and parasitic elements in the power supply and its environment. Its magnitude and phase vary with frequency.

Manuscript received February 26, 2003; revised July 24, 2003. Recommended by Associate Editor P. Tenti.

The authors are with the Department of Electrical and Computer Engineering, Queen's University, Kingston K7L 3N6, ON, Canada (e-mail: sheng.ye@ece.queensu.ca; wilsoneberle@wilsoneberle.com; yanfei.liu@ece.queensu.ca).

Digital Object Identifier 10.1109/TPEL.2004.836629

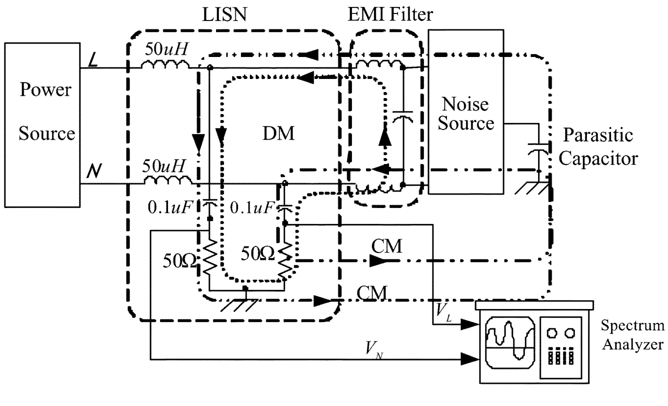

Fig. 1. EMI noise measurement test setup.

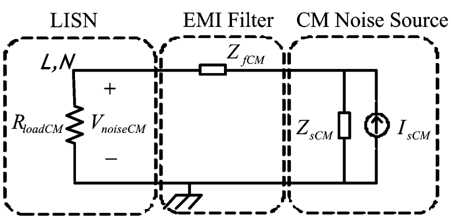

Fig. 2. CM noise equivalent circuit of a SPS with a CM inductor.

In this section, the interaction between the noise impedance of the noise source and the output impedance of the EMI filter is analyzed. Experimental results are presented to verify the theory for a commercially available, telecommunications, $1/2$ brick size, isolated dc–dc power module with a nominal input voltage of 48 V, and an output voltage of 3.3 V at a full load current of 30 A. A power combiner was used in the measurements to separate the CM and DM noise spectrum from the total line noise spectrum [3], so that the impact of the CM and DM noise impedances could be considered independently.

In subsection A, the impact of the CM noise impedance is considered and in subsection B, the impact of the DM noise impedance is considered. It will be demonstrated that if the parameters of the EMI filter are not selected properly, the EMI filter can amplify noise at certain frequencies.

A. Impact of the CM Noise Impedance

The attenuation of an EMI filter is defined by

$$A_T = \frac{V_{\text{noise without filter}}}{V_{\text{noise with filter}}}. \tag{1}$$

$V_{\text{noise without filter}}$ is measured at the LISN output as shown in Fig. 1 when no CM inductor is added, which corresponds to the situation when no EMI filter is added. $V_{\text{noise with filter}}$ is measured at the LISN output when a CM inductor is added. The filter attenuation, A_T, is a function of frequency, so measurements must be taken, so that it can be calculated at several frequency points.

In order to simplify the analysis, it was assumed that: 1) the CM filter only consisted of a CM inductor, 2) the CM inductor only suppressed the CM noise, and 3) the CM noise current only conducted from noise source to earth. The CM equivalent circuit is obtained when a CM inductor is added to the input of the SPS, which is labeled "noise source" in Fig. 1. The equivalent circuit is shown in Fig. 2. The impedance of the CM inductor is Z_{fCM}. R_{loadCM} is the equivalent resistance of the LISN. I_{sCM} represents the SPS noise source and Z_{sCM} represents the noise source impedance.

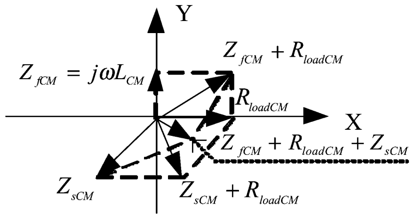

Fig. 3. Vector explanation of (4).

The noise voltage V_{noise} across R_{loadCM}, before and after the CM inductor is added, can be expressed by (2) as $V_{\text{noise without filter}}$ and (3) as $V_{\text{noise with filter}}$, respectively

$$V_{\text{noise without filter}} = \frac{R_{\text{loadCM}} Z_{\text{sCM}}}{R_{\text{loadCM}} + Z_{\text{sCM}}} I_{\text{sCM}} \tag{2}$$

$$V_{\text{noise with filter}} = \frac{R_{\text{loadCM}} Z_{\text{sCM}}}{R_{\text{load CM}} + Z_{\text{sCM}} + Z_{\text{fCM}}} I_{\text{sCM}}. \tag{3}$$

If (4) is satisfied, V_{noise} will be amplified after a CM inductor is added

$$|R_{\text{loadCM}} + Z_{\text{sCM}} + Z_{\text{fCM}}| < |R_{\text{loadCM}} + Z_{\text{sCM}}|. \tag{4}$$

In Fig. 3, (4) is illustrated for possible vector magnitudes of the parameters $R_{\text{loadCM}}, Z_{\text{fCM}}$, and Z_{sCM}.

It can be noted from Fig. 3, that under certain conditions, the amplitude of vectors $R_{\text{loadCM}} + Z_{\text{fCM}}$ and Z_{sCM} can be nearly equal with a phase difference of approximately 180°. Under these conditions, the filter amplifies the noise. At high frequencies, the inductance dominates ($Z_{\text{fCM}} \gg R_{\text{loadCM}}$ and $Z_{\text{fCM}} \gg Z_{\text{sCM}}$). At these high frequencies, the CM inductor can effectively suppress the CM noise spectrum. The CM noise spectrum before and after a CM inductor was added to the input of the SPS is illustrated in Fig. 4.

From the test results, we can see that the noise at 583 kHz was amplified, but at higher frequencies the noise was effectively suppressed. This demonstrates that the EMI filter should be designed properly in order to attenuate the noise for the entire frequency range.

In Fig. 4, the FCC 15 class A standards for conducted EMI have been included (top line) and a 3-dB limit is shown below the FCC class A standards. It is generally desirable to design a filter so that its noise spectrum is below the 3-dB limit to account for varying environmental conditions and component tolerances.

It is worth noting that more complex topologies for a CM filter can be used, but if the CM filter is not designed to match the CM noise impedance, the effects of the deteriorated impact of the EMI filter will still exist.

B. Impact of the DM Noise Impedance

In order to simplify the analysis, it was assumed that 1) the DM filter only consisted of an X capacitor, 2) the X capacitor only suppressed the DM noise, and 3) the DM current only

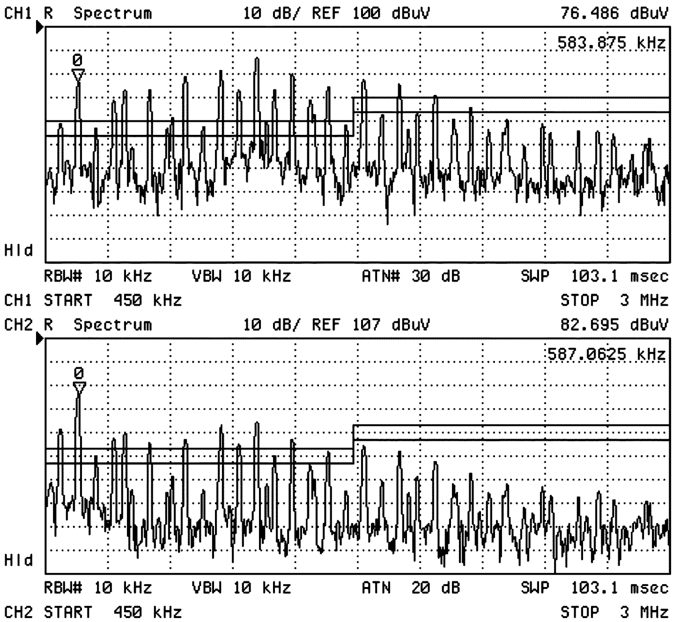

Fig. 4. CM noise test results before (CH1) and after (CH2) a CM inductor was added.

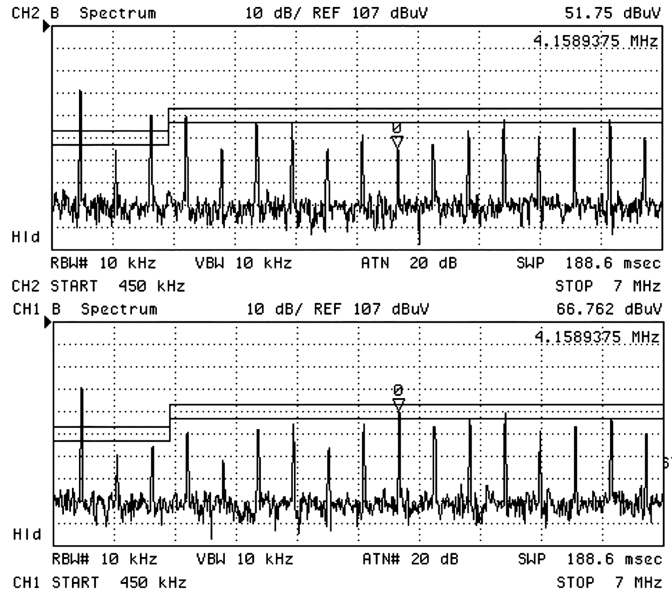

Fig. 6. Test results illustrating amplification of DM noise before (CH2) and after (CH1) an X capacitor was added.

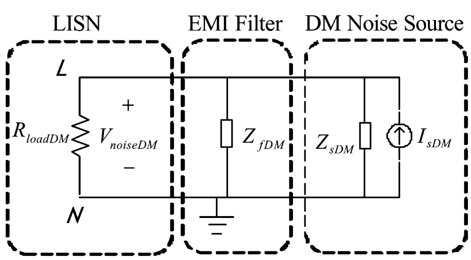

Fig. 5. DM noise equivalent circuit after an X capacitor is added.

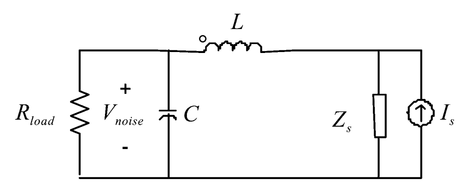

Fig. 7. Noise equivalent circuit with the inductor at the input of the SPS.

conducted from noise source to power ground. Given these assumptions, the same method was used to analyze the DM noise impedance's impact.

The DM noise equivalent circuit is illustrated in Fig. 5. An X capacitor was added to the input of SPS. Using (1), and the equivalent circuit in Fig. 5, we obtain (5), which simplifies to (6) for $Z_{\mathrm{sDM}} \ll R_{\mathrm{loadDM}}$, where Z_{sDM} is the DM noise impedance of the SPS and Z_{fDM} is X capacitor's impedance.

$$|A_{\mathrm{TDM}}| = \left|1 + \frac{R_{\mathrm{loadDM}} Z_{\mathrm{sDM}}}{Z_{\mathrm{fDM}}(R_{\mathrm{loadDM}} + Z_{\mathrm{sDM}})}\right| \tag{5}$$

$$|A_{\mathrm{TDM}}| \approx \left|1 + \frac{Z_{\mathrm{sDM}}}{Z_{\mathrm{fDM}}}\right|. \tag{6}$$

If $-1 < Z_{\mathrm{sDM}}/Z_{\mathrm{fDM}} < 0$, the attenuation is less than one, and the DM noise is amplified. This phenomenon is illustrated in Fig. 6, where the DM noise spectrum at 4.15 MHz was amplified when an X capacitor was added to the input of the SPS.

Similar to the case for CM filter design, more complex topologies for the DM filter can be used. However, if the DM filter is not designed to match the DM noise impedance, the effects of the deteriorated impact of the EMI filter will still exist.

From the above analysis and experimental results, for both the CM and DM cases, we can see that in order to effectively suppress the EMI noise, the EMI filter must be designed to match the noise impedance. If the inductor faces the input of the SPS, the inductor's impedance should be much larger than the noise impedance, in order to effectively suppress the noise. The opposite is true if the capacitor faces the input of the SPS, namely the capacitor's impedance should be much smaller than the noise impedance, so that the noise may be suppressed via the capacitor and not the parallel noise source impedance. This can be demonstrated by considering the two common filter configurations illustrated in Fig. 7, where the inductor faces the input of the SPS, and in Fig. 8, where the capacitor faces the input of the SPS.

For the configuration of Fig. 7, if it is assumed that the inductors impedance is much larger than the noise impedance, then the phase angle of the noise impedance can be neglected and the worst case attenuation occurs when the noise impedance is large. Therefore, it is proposed that if the maximum magnitude of the noise impedance, $|Z_s|_{\mathrm{Max}}$, can be easily determined, then the EMI filter can be effectively designed using the maximum magnitude of the noise impedance.

For the configuration of Fig. 8, if it is assumed that the capacitors impedance is much smaller than the noise impedance, then the phase angle of the noise impedance can be neglected and the worst case attenuation occurs when the noise impedance is small. Therefore, it is proposed that if the minimum magnitude of the noise impedance, $|Z_s|_{\mathrm{Min}}$, can be easily determined, then the EMI filter can be effectively designed using the minimum magnitude of the noise impedance.

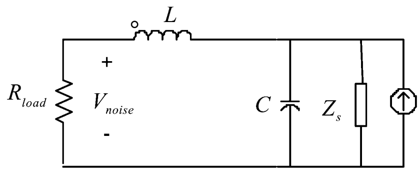

Fig. 8. Noise equivalent circuit with the capacitor at the input of the SPS.

IV. Determination of the Maximum and Minimum CM and DM Noise Impedances

It has been demonstrated that the noise impedance has a significant impact on the attenuation of the EMI filter. In order to effectively attenuate the EMI noise over the frequency range of interest, the EMI filter must be designed to match the noise impedance. However, the phase angle and amplitude of the noise impedance of a SPS varies by frequency. Furthermore, it is difficult to measure the noise impedance's phase angle and amplitude accurately over a wide frequency range, such as that required by the FCC 15 (0.45 to 30 MHz).

It was proposed in Section III, that 1) if the maximum possible amplitude and the minimum possible amplitude of the noise impedance can be determined and 2) if the EMI filter components are selected properly, then the EMI filter can be designed effectively. In addition, the task of measuring the maximum and minimum amplitude of the noise impedance is much easier. The measurement methods are summarized below. For the measurements, a power combiner was used to separate the CM and DM noise spectrum from the total line noise spectrum.

A. Determining the Maximum Possible Value and Minimum Possible Value of the CM Noise Impedance

For the CM noise impedance measurement, it was assumed that: 1) the CM inductor only suppresses the CM mode noise and 2) the CM noise current only conducts from the noise source to earth.

In order to measure the maximum possible value and minimum possible value of the CM noise impedance, a test inductor was added to the input of the SPS. The measurement test setup is illustrated in Fig. 9. The circuit in Fig. 9 can be further simplified to the CM equivalent circuit, illustrated in Fig. 2. Using the equivalent circuit in Fig. 2 and (1), (7) can be derived and simplified as (8), where $Z_{\rm fCM}$ is the impedance of the CM inductor and $R_{\rm loadCM} = 25\ \Omega$ is the LISN parallel equivalent resistance

$$A_{\rm TCM} = \frac{\frac{R_{\rm loadCM} Z_{\rm sCM}}{R_{\rm loadCM}+Z_{\rm sCM}} I_{\rm sCM}}{\frac{Z_{\rm sCM}}{R_{\rm loadCM}+Z_{\rm sCM}+Z_{\rm fCM}} I_{\rm sCM} R_{\rm loadCM}} \tag{7}$$

$$A_{\rm TCM} = 1 + \frac{Z_{\rm fCM}}{R_{\rm loadCM}+Z_{\rm sCM}}. \tag{8}$$

From (8), the following relationship is obtained:

$$|R_{\rm loadCM}+Z_{\rm sCM}| = \frac{|Z_{\rm fCM}|}{|A_{\rm TCM}-1|}. \tag{9}$$

It is noted that $A_{\rm TCM}$ is a complex quantity and only $|A_{\rm TCM}|$ can be easily measured. The objective is to find the maximum and minimum noise source impedances $|Z_{\rm sCM}|_{\rm Max}$ and

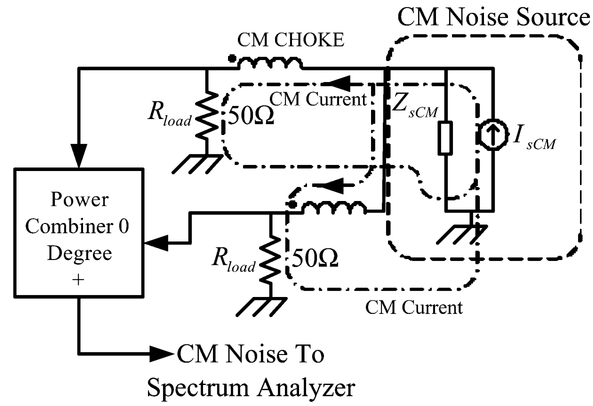

Fig. 9. CM noise impedance measurement test setup.

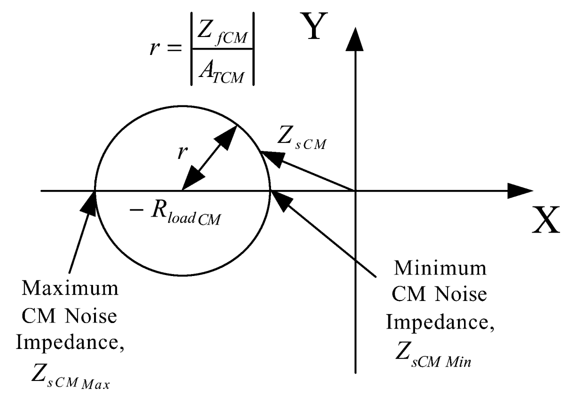

Fig. 10. Graphical illustration of (10).

$|Z_{\rm sCM}|_{\rm Min}$, respectively. For $A_{\rm TCM} \gg 1$, the relationship given by (10) is derived from (9)

$$|R_{\rm loadCM}+Z_{\rm sCM}| \approx \frac{|Z_{\rm fCM}|}{|A_{\rm TCM}|}. \tag{10}$$

In (10), $Z_{\rm sCM}$ is the CM noise impedance and $R_{\rm loadCM}(= 25\ \Omega)$ is the LISN CM load resistance. $A_{\rm TCM}$ is the CM noise attenuation measured after a test CM inductor was added. $Z_{\rm fCM}$ is the impedance of the test CM inductor at the test frequency point. From (10), it is clear that $|Z_{\rm fCM}/A_{\rm TCM}|$ is a fixed real number. Furthermore, suppose $|Z_{\rm fCM}/A_{\rm TCM}|$ is the radius r. Then in (10), the only unknown variable is $Z_{\rm sCM}$, which is a complex number. If we let $Z_{\rm sCM}$ represent a complex number as $Z_{\rm sCM} = x + jy$, then (10) can be expressed by (11), where it is clear that (11) represents a circle centered at $-R_{\rm loadCM}$ with radius $r = |Z_{\rm fCM}/A_{\rm TCM}|$. This circle is illustrated in Fig. 10. The maximum and the minimum magnitude of the noise impedance can be derived easily From Fig. 10

$$\begin{aligned}|(R_{\rm loadCM}+x)+jy| = r &\rightarrow \sqrt{(R_{\rm loadCM}+x)^2+y^2} \\ &= r \rightarrow (R_{\rm loadCM}+x)^2+y^2 = r^2.\end{aligned} \tag{11}$$

It is clear from Fig. 10, that the maximum CM noise impedance $Z_{\rm sCMMax}$ is on the real axis on the left side of the circle. The minimum CM noise impedance $Z_{\rm sCMMin}$ is on the real axis on the right side of the circle. Therefore, using Fig. 10

and (9), the maximum possible magnitude and minimum possible magnitude of CM noise impedances for 1) $|A_{\rm TCM}| \geq 10$ and 2) $|A_{\rm TCM}| < 10$ are approximated as follows.

1) When $|A_{\rm TCM}| \geq 10$

$$|Z_{\rm sCM}|_{\rm Max} \approx \left| R_{\rm loadCM} + \frac{|Z_{\rm fCM}|}{|A_{\rm TCM}|} \right| \tag{12}$$

$$|Z_{\rm sCM}|_{\rm Min} \approx \left| R_{\rm loadCM} - \frac{|Z_{\rm fCM}|}{|A_{\rm TCM}|} \right|. \tag{13}$$

2) When $|A_{\rm TCM}| < 10$

$$|Z_{\rm sCM}|_{\rm Max} \approx \left| R_{\rm loadCM} + \left| \frac{Z_{\rm fCM}}{|A_{\rm TCM}| - 1} \right| \right| \tag{14}$$

$$|Z_{\rm sCM}|_{\rm Min} \approx \left| R_{\rm loadCM} - \left| \frac{Z_{\rm fCM}}{|A_{\rm TCM}| + 1} \right| \right|. \tag{15}$$

For example, at full load the CM noise spike of the SPS at 1 MHz was 70 dB. After a test CM inductor was added, such that the attenuation was greater than one, the CM noise at 1 MHz was 50 dB, then

$$|A_{\rm TCM}| = 10^{\frac{70-50}{20}} = 10.$$

Using an impedance analyzer, the CM inductor's impedance was measured to be 5 kΩ at 1 MHz. $|Z_{\rm sCM}|_{\rm Max}$ and $|Z_{\rm sCM}|_{\rm Min}$ were calculated to be 525 and 475 Ω using (12) and (13), respectively. Typically, the CM noise impedance varies with frequency, so some points in the frequency range of interest were selected and then the maximum possible value and minimum possible value of the CM noise impedance were calculated at these frequency points.

B. Determining the Maximum Possible Value and Minimum Possible Value of the DM Noise Impedance

For the DM noise impedance measurement, it was assumed that 1) the X capacitor only suppressed the DM noise and 2) the DM noise impedance $Z_{\rm sDM}$ was smaller than LISN equivalent resistance of 100 Ω, (typically, $|Z_{\rm sDM}| \ll 100$ Ω), and 3) the DM noise current only conducted from the noise source to power ground.

To measure the maximum and minimum DM noise impedance, a test X capacitor was added to the input of the SPS under test. The test setup is illustrated in Fig. 11.

The circuit in Fig. 11 can be further simplified to the circuit shown in Fig. 5. Using the DM equivalent circuit of Fig. 5 and (1), (16) was derived and approximated as (17), where $|Z_{\rm sDM}| \ll R_{\rm loadDM} = 100$ Ω and $Z_{\rm fDM}$ is the impedance of the X capacitor

$$|A_{\rm TDM}| = \left| \frac{\frac{R_{\rm loadDM} Z_{\rm sDM}}{R_{\rm loadDM} + Z_{\rm sDM}} I_{\rm sDM}}{\frac{R_{\rm loadDM} Z_{\rm sDM} Z_{\rm fDM}}{R_{\rm loadDM} Z_{\rm fDM} + Z_{\rm sDM} Z_{\rm fDM} + R_{\rm loadDM} Z_{\rm sDM}} I_{\rm sDM}} \right| \tag{16}$$

$$|A_{\rm TDM}| \approx \left| 1 + \frac{Z_{\rm sDM}}{Z_{\rm fDM}} \right| \tag{17}$$

$$|Z_{\rm sDM}|_{\rm Min} = |Z_{\rm fDM}| \, ||A_{\rm TDM}| - 1| \tag{18}$$

$$|Z_{\rm sDM}|_{\rm Max} = |Z_{\rm fDM}| \, ||A_{\rm TDM}| + 1|. \tag{19}$$

It is noted that $A_{\rm TDM}$ is a complex quantity and only $|A_{\rm TDM}|$ can be easily measured. The maximum and minimum value

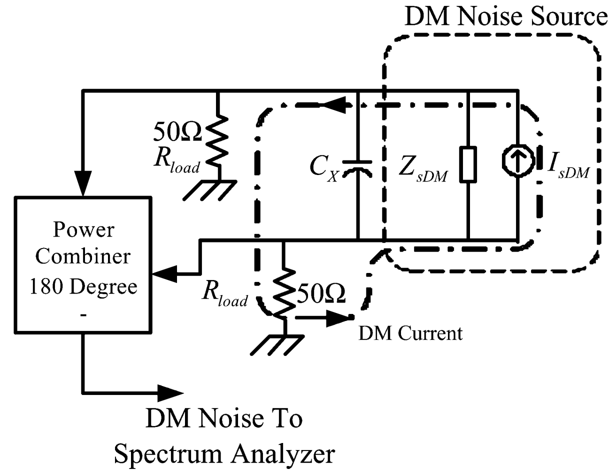

Fig. 11. DM noise impedance measurement test setup.

DM noise impedance measurement was similar to the CM noise impedance measurement. Equations (18) and (19) were used to calculate the maximum and minimum DM noise impedances. After measuring the maximum possible value and minimum possible value of the CM and DM noise impedances, the EMI filter topology and components were selected based on the maximum or minimum value of the CM and DM noise impedances, for whichever yielded the least or worst case attenuation.

V. EMI Filter Design

In this section, a method to design an EMI filter using the maximum and minimum CM and DM noise impedances is introduced. The dc–dc power supply described in Section III is used as an example. The objective was to design an EMI filter, so that the SPS would pass the FCC 15 Class B regulations for conducted EMI. The CM and DM filters were designed separately. The maximum or minimum worst case noise impedance was considered for each filter. After completion of the CM and DM filters, they were put together to make the complete filter. The procedure to design the EMI filter is summarized as follows.

1) Test the CM and DM noise spectrum of the SPS.
2) Measure the noise voltage, $V_{\rm noise}$, with and without a simple filter (e.g., a capacitor), and then use the attenuation to calculate the maximum CM and DM noise impedances for the frequency range under consideration (0.45–30 MHz for the FCC 15).
3) Design the EMI filter using the maximum magnitude, or minimum magnitude of the noise impedance, which ever yields the least attenuation.
4) Test the completed EMI filter.

The CM and DM noise spectra of the unfiltered dc–dc SPS, operating at full load, are illustrated in Figs. 12 and 13, respectively. The FCC 15 Class B standards are indicated by the top horizontal line, and the second line is a 3-dB margin below the FCC 15 Class B line.

From the test results, it is noted that the CM noise was the dominant factor. Furthermore, the largest noise spikes occurred in the range from 0.45 to 2 MHz. Therefore, the CM noise impedance measurements were focused within this range. Cal-

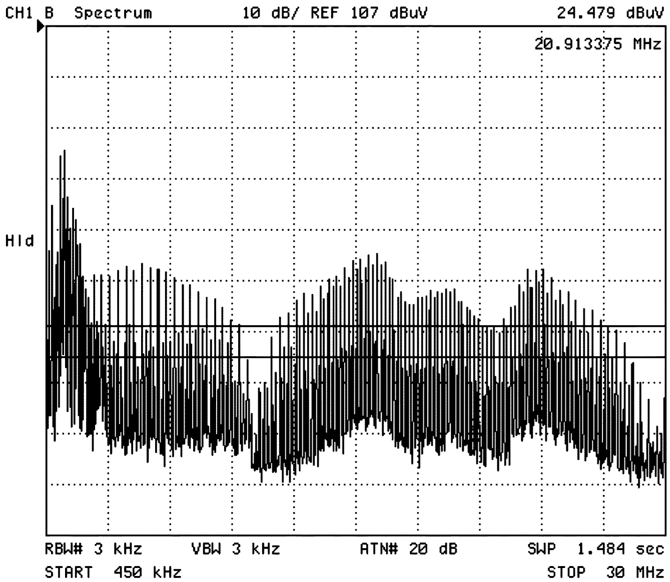

Fig. 12. CM noise spectrum of the dc–dc SPS without a CM filter.

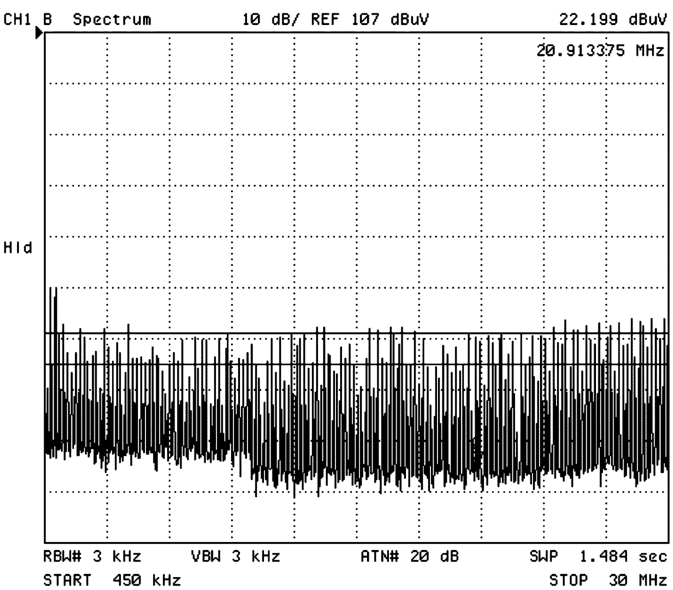

Fig. 13. DM noise spectrum of the dc–dc SPS without a DM filter.

culations were made at different frequency points using measurements of the noise voltage V_{noiseCM} along with (1) and (12)–(15). The resulting impedances were plotted as shown in Fig. 14.

The maximum possible value and minimum possible value of the DM noise impedance from 0.45 to 2.5 MHz were calculated at different frequency points using measurements of the noise voltage V_{noiseDM} along with (1), (18), and (19). The resulting impedances were calculated as shown in Fig. 15.

A. CM Filter Design

In order to design the CM filter we need to know: 1) the attenuation required to make the CM noise spectrum pass the EMI standards at the frequencies of interest and 2) the worst case, maximum, or minimum noise impedance for the frequency range of interest.

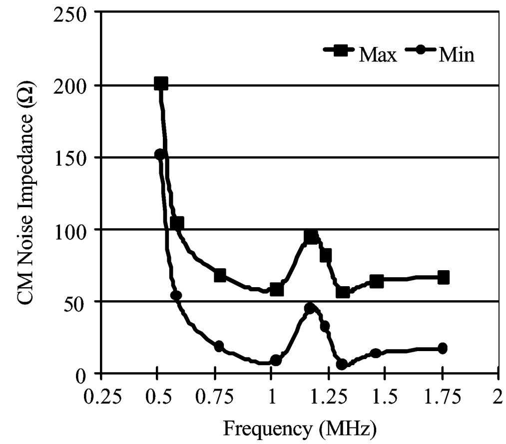

Fig. 14. Maximum value and minimum value of the CM noise impedance from 0.45 to 2 MHz.

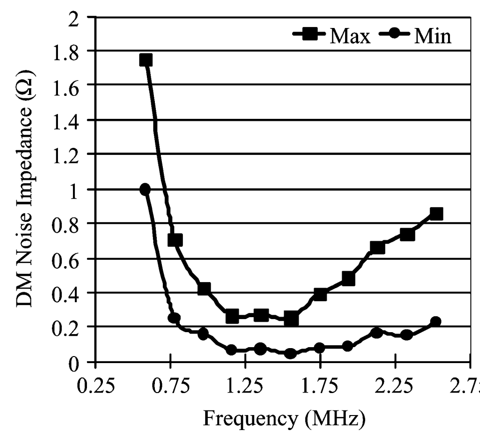

Fig. 15. Maximum value and minimum value of the DM noise impedance from 0.45 to 2.5 MHz.

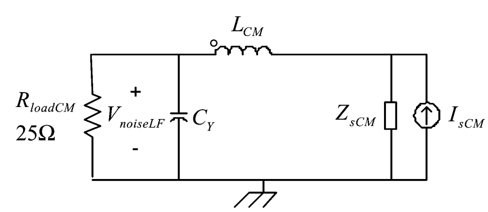

Fig. 16. CM noise equivalent circuit with the CM inductor at the input of the SPS.

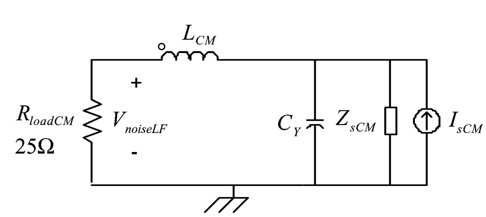

Fig. 17. CM noise equivalent circuit with the Y capacitor at the input of the SPS.

For the CM part of the EMI filter, two basic topologies can be selected. In the first topology, the CM inductor faces the input of the SPS, as illustrated in Fig. 16. In the second topology, the Y capacitor faces the input of the SPS, as illustrated in Fig. 17. Using the equivalent circuits of Fig. 16 and Fig. 17, the CM

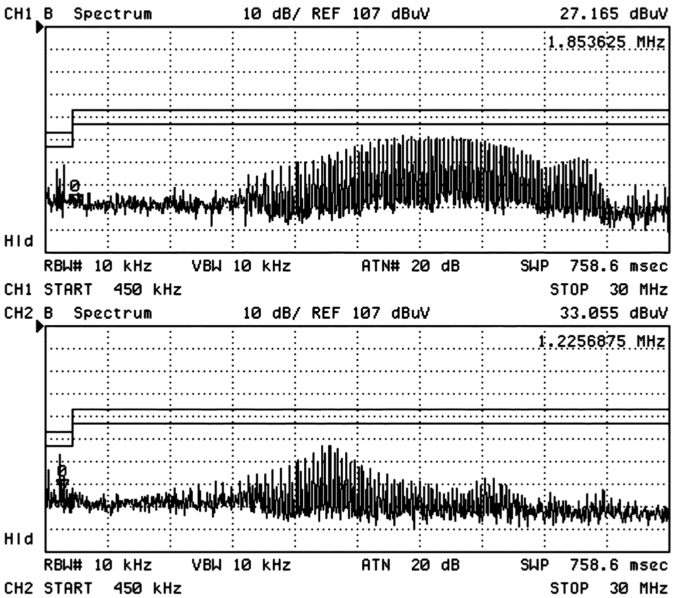

Fig. 18. CM noise spectrum test results for the topologies of Fig. 16 (CH2) with the inductor at the input and Fig. 17 (CH1) with the capacitor at the input.

noise voltage across R_{loadCM} was calculated when the filter was added.

Two topologies were tested. The test results are shown in Fig. 18. For the test, the CM inductance used was 100 μH and the Y capacitor used was 330 nF. From the results, it was concluded that the topology of Fig. 16 should be used because it provided more attenuation at high frequencies than the topology shown in Fig. 17. This result also emphasizes the fact that noise impedance has a significant effect on the performance of the EMI filter.

In order to determine the lowest corner frequency required for the CM filter, (20) was used

$$f_c = \frac{F_0}{\sqrt{A_{\mathrm{TCMreq}}}}. \tag{20}$$

A_{TCMreq} is the required attenuation at frequency F_0, and f_c is the corner frequency of the CM filter. The CM attenuation required for the SPS to pass the FCC 15 Class B standards with a 3-dB margin was plotted over the frequency range from 0.5–1.5 MHz as shown in Fig. 19. Equation (20) was evaluated at each point for the data presented in Fig. 19. The results are shown in Fig. 20. The lowest calculated filter corner frequency was $f_c = 94$ kHz, using $F_0 = 583$ kHz at $A_{\mathrm{TCMreq}} = 38$.

To select the value of the CM inductor, the maximum noise impedance was used because it provides the least attenuation for the filter in Fig. 16, where the inductor faces the input of the SPS. From Fig. 14, it is noted that the maximum magnitude of the CM noise impedance is 205 Ω. If the phase angle of the noise impedance is neglected and we want to guarantee that CM noise impedance has little effect on the performance of the EMI filter, the impedance of the CM inductor at the frequency of interest must be much larger than the maximum magnitude of the CM noise impedance.

In fact, if we want to make sure the desired attenuation is achieved, the CM inductor's impedance must be at least double

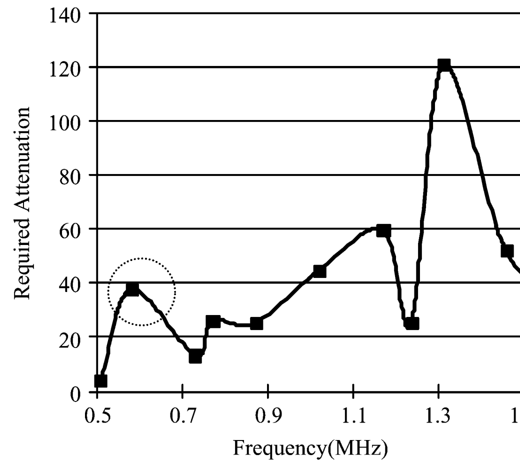

Fig. 19. Attenuation required for the CM Noise Spectrum to pass FCC Class B standards with a 3-dB margin.

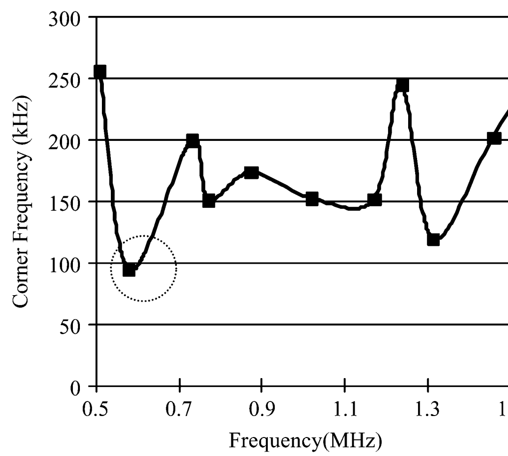

Fig. 20. CM filter corner frequency required for the CM Noise Spectrum to pass FCC Class B standards.

the maximum magnitude of the CM noise impedance. Therefore, the CM inductor's impedance at F_0 must be larger than $2 \times 205\,\Omega = 410\,\Omega$, which corresponds to an inductance greater than $2 \times 55.9\ \mu\mathrm{H} = 111.8\ \mu\mathrm{H}$. The inductance chosen can be any reasonable value above 111.8 μH, so in order to leave some margin, a 200 μH inductance was selected. The impedance of this CM inductor at 583 kHz is 732 Ω which is approximately three times the maximum magnitude of the CM noise impedance.

Ignoring the phase angle of the CM noise impedance (i.e., considering the CM noise impedance as purely resistive), the attenuation of the topology in Fig. 16, can be expressed by (21) where V_1 and V_2 are given by (22) and (23), respectively. Parameters Z_1 and Z_2 are given by (24) and (25), respectively

$$|A_{\mathrm{TCM}}| = \left|\frac{V_2}{V_1}\right| \tag{21}$$

$$V_1 = \frac{Z_1 Z_2}{(Z_{\mathrm{LCM}} + Z_1)} I_{\mathrm{sCM}} \tag{22}$$

$$V_2 = \frac{R_{\mathrm{load}} Z_{\mathrm{sCM}}}{R_{\mathrm{load}} + Z_{\mathrm{sCM}}} I_{\mathrm{sCM}} \tag{23}$$

$$Z_1 = \frac{R_{\mathrm{load}} Z_{\mathrm{CY}}}{R_{\mathrm{Load}} + Z_{\mathrm{CY}}} \tag{24}$$

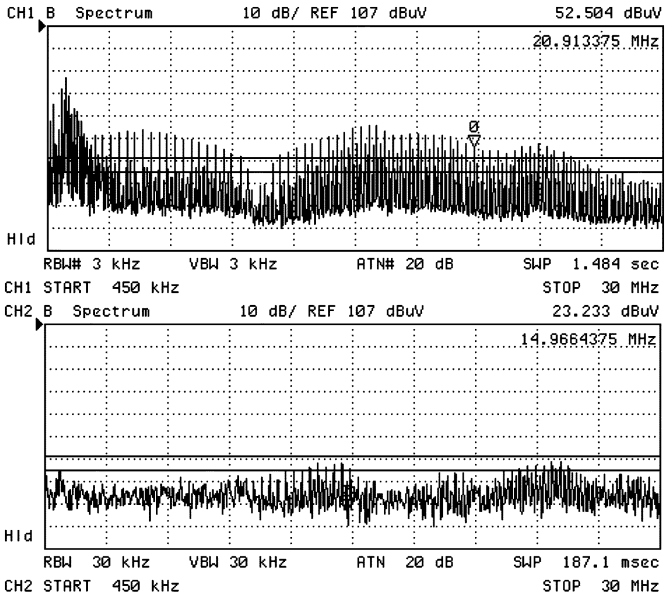

Fig. 21. Test results of the CM noise spectrum before (CH1) and after (CH2) the CM filter designed based on maximum noise impedance was added.

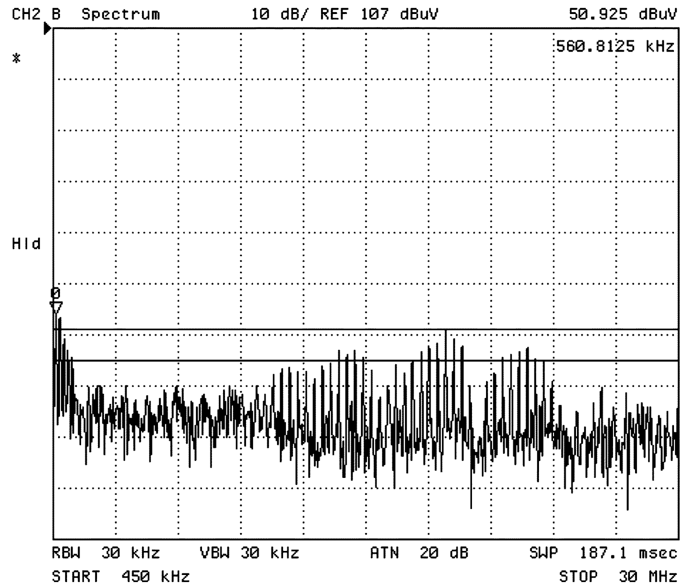

Fig. 22. Test results of the CM filter based on the ideal case.

$$Z_2 = (Z_{\rm LCM} + Z_1)\left(\frac{Z_{\rm sCM}}{Z_{\rm sCM} + Z_1 + Z_{\rm LCM}}\right). \quad (25)$$

$Z_{\rm LCM}$ is the impedance of the CM inductor. $Z_{\rm CY}$ is the impedance of the Y capacitor. V_2 is the voltage across the LISN equivalent resistor shown in Fig. 16 and V_1 is the noise voltage across the LISN resistor without the CM filter.

The final step in the filter design is to select the capacitance. A capacitance of 136 nF was selected using two C_Y capacitors of 68 nF each in parallel. Using this capacitance and (21), the calculated attenuation of the filter at 583 kHz was 41, which was greater than the required attenuation of 38. Fig. 21 shows the experimental results of the CM spectrum with (CH2) and without (CH1) the CM filter, where the filter was designed using the maximum noise impedance.

It is noted that the SPS with the CM filter passed the FCC 15 Class B requirements over the required frequency range and the attenuation achieved was greater than the 3-dB margin over most of the frequency range.

If the capacitance was selected based on an ideal LC filter design, the calculated capacitance required would be 14.3 nF using (26). The closest available capacitance is 16.4 nF (2 × 8.2 nF in parallel)

$$f_c = \frac{1}{2\pi\sqrt{L_{\rm CM}C_Y}}. \quad (26)$$

Then, using (21), with the parameters as follows $C_Y = 16.4$ nF, $R_{\rm loadCM} = 25\ \Omega, L_{\rm CM} = 200\ \mu$H, and $Z_{\rm sCM} = 205\ \Omega$, the calculated attenuation is 5.9 at 583 kHz. This is less then the required attenuation, $A_{\rm TreqCM} = 38$. Fig. 22 shows the test results for the filter design based on the ideal case, using $L_{\rm CM} = 200\ \mu$H and $C_Y = 16.4$ nF. It is obvious that this filter does not meet the FCC Class B requirements at approximately 560 kHz.

From the above analysis, it is clear that neglecting the noise impedance leads a designer to design a filter that will not meet the requirements. Neglecting the noise impedance, the selected Y capacitance is 16.4 nF, but when the noise impedance is taken into account, the selected capacitance of 136 nF is nearly ten times larger. The experiment results also verified this conclusion. From above analysis and experimental results it is again demonstrated that the noise impedance has a significant effect on the performance of the EMI filter.

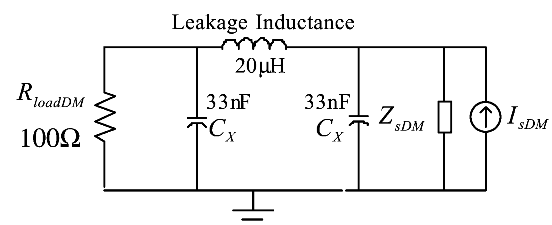

Fig. 23. DM noise equivalent circuit including the π DM filter topology.

B. DM Filter Design

The DM filter design method is similar to that of the CM filter. In order to design the DM filter we need to know: 1) the attenuation required to make the DM noise spectrum pass the EMI standards at the frequencies of interest and 2) the maximum possible value and minimum possible value of the noise impedance for the frequency range of interest.

A π topology was selected to suppress the DM noise, because this topology provides better performance than other simple topologies such as the LC topology. The topology, along with the noise source, its impedance and $R_{\rm loadDM}$, is displayed in Fig. 23.

Since an X capacitor was used at the input of the SPS, the minimum DM noise impedance was used for the filter design. The attenuation of this topology can be expressed using (27), where $Z_{\rm Cl}$ and $Z_{\rm Cs}$ are given by (28) and (29), respectively. In (28) and (29), $Z_{\rm CX}$ is the impedance of the X capacitor and

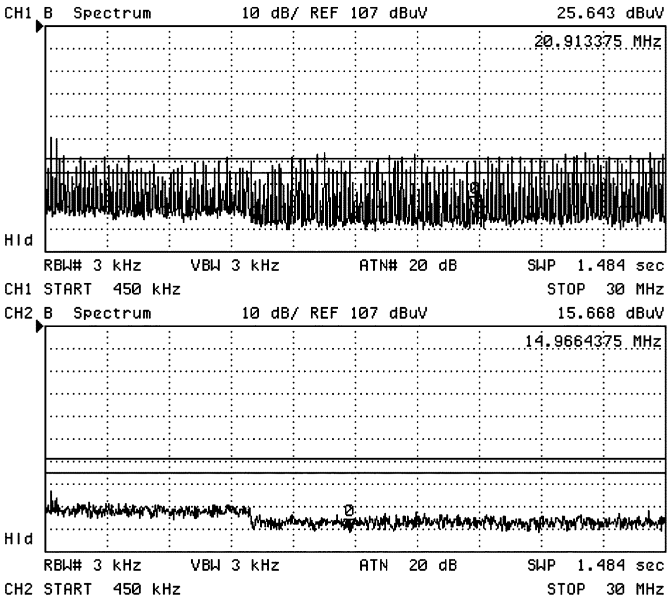

Fig. 24. Test results for DM noise spectrum before (CH1) and after (CH2) the PI filter was added with the FCC Class B limits indicated.

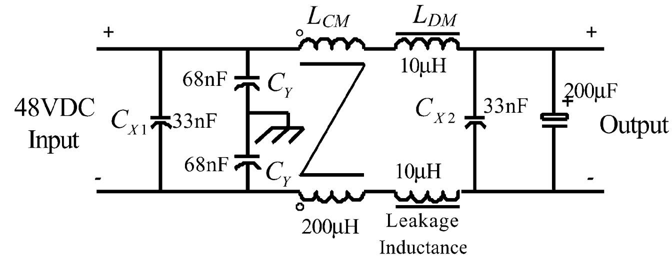

Fig. 25. Complete EMI filter containing the CM and DM filters for the dc–dc SPS.

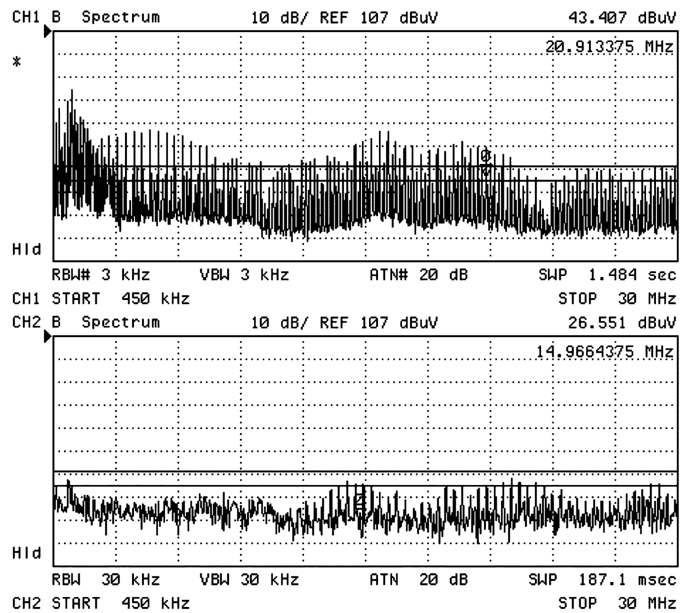

Fig. 26. Test results of the total noise spectrum before (CH1) and after (CH2) the EMI filter was added to the input of the dc–dc SPS with the FCC Class B limits indicated.

in (27), Z_{LDM} is the impedance of the differential mode inductance. In (27) and (28), R_{loadDM} is the LISN equivalent load resistance of 100 Ω

$$|A_{\mathrm{TDM}}| = \left| \frac{R_{\mathrm{loadDM}} Z_{\mathrm{sDM}} (Z_{\mathrm{Cl}} + Z_{\mathrm{LDM}} + Z_{\mathrm{Cs}})}{(R_{\mathrm{loadDM}} + Z_{\mathrm{sDM}}) Z_{\mathrm{Cs}} Z_{\mathrm{Cl}}} \right| \quad (27)$$

$$Z_{\mathrm{Cl}} = \frac{R_{\mathrm{loadCM}} Z_{\mathrm{CX}}}{R_{\mathrm{loadCM}} + Z_{\mathrm{CX}}} \quad (28)$$

$$Z_{\mathrm{Cs}} = \frac{Z_{\mathrm{CX}} Z_{\mathrm{sDM}}}{Z_{\mathrm{CX}} + Z_{\mathrm{sDM}}}. \quad (29)$$

Using the experimental results given in Fig. 13, the lowest corner frequency required was at $F_0 = 583$ kHz. At this frequency, the attenuation needed was 4.5. It should be noted that the leakage inductance of the CM inductor was used as the DM inductance, so only one inductor was required to meet the attenuation requirements for the CM noise and the DM noise. Using (27), along with $L_{\mathrm{DM}} = 20\ \mu$H, $|Z_{\mathrm{sDM}}|_{\mathrm{Min}} = 0.06\ \Omega$, and $C_X = 33$ nF, the calculated attenuation $|A_{\mathrm{TDM}}|$ was 7.87 at $F_0 = 583$ kHz, which was greater than the required attenuation of 4.5. The test results of the DM noise spectrum before (CH1) and after (CH2) the DM filter was added are shown in Fig. 24. It is clear that the DM filter exceeded the FCC 15 Class B specifications over the entire frequency range by more than 3 dB.

Finally, the CM and DM filters were assembled together. The final EMI filter is illustrated in Fig. 25. A 200-μF electrolytic capacitor was added to the output of the filter to ensure that the EMI filter would not destabilize the feedback loop of the SPS [4]. Since the resonant frequency of this electrolytic capacitor is relatively low, it does not affect the filter design. The test results for the filter are shown in Fig. 26. From the test results, it can be noted that the filter allows the SPS to pass the FCC 15 Class B requirements for conducted EMI.

C. Design Considerations

When the method proposed in this paper is used to select components, the resonant frequency of the components should also be considered because at high frequencies the ESR, ESL, and end-to-end capacitance of the components cannot be neglected. At high frequencies, capacitors become inductive and inductors become capacitive. Therefore, when selecting components, we should select the components which have as high resonant frequencies as possible. Other good engineering practices, such as inductive beads, high frequency capacitors, can also be used to attenuate the high frequency EMI noise. Attention should also be paid to the layout of the EMI filter to avoid noise coupling.

Fortunately, it is observed that the high frequency noise is not a major issue to pass the EMI requirements. In this paper, the selected capacitor and inductor have high enough resonant frequency and are sufficient for the power converter to meet the EMI standards. In some special cases where the required attenuation is very large, multistage EMI filters should be employed, where smaller capacitors and inductors with higher resonant frequencies can be used. The design method is summarized in the flow chart illustrated in Fig. 27.

VI. Extending the Method to Design EMI Filters for AC–DC SPS

The proposed method was used to design an EMI filter for an ac–dc power supply. Experimental results are presented for

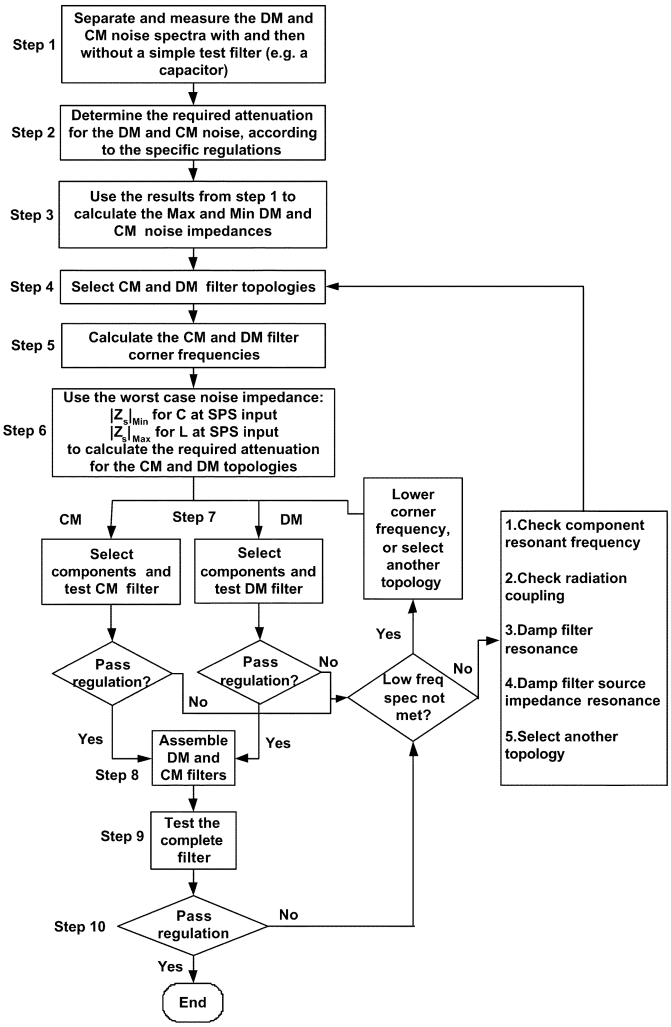

Fig. 27. Flow chart of the proposed design method.

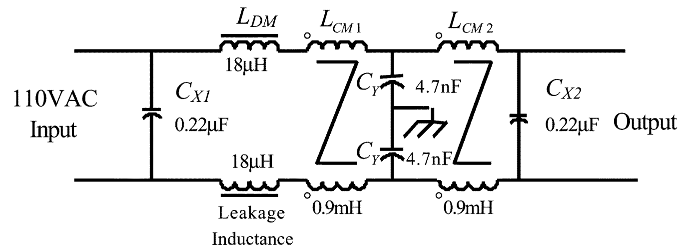

Fig. 28. Complete EMI filter containing the DM and CM filters for the ac–dc SPS.

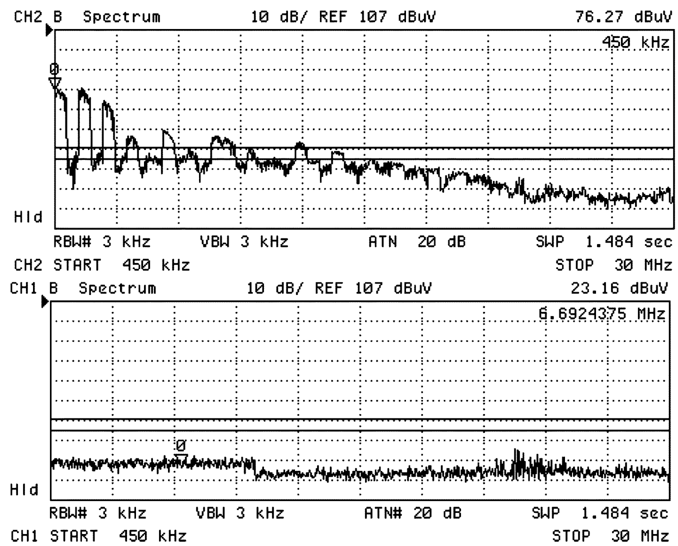

Fig. 29. Test results of the total noise spectrum before (CH1) and after (CH2) the EMI filter was added to the input of the ac–dc SPS with the FCC Class B limits indicated.

a commercially available, ac–dc power module with a nominal input voltage of 120 V_{RMS}, and an output voltage of 5.1 V_{DC} at a full load current of 22 A.

After measuring the DM and CM noise spectrum and calculating the noise impedance, the filter topology was selected. The topology is illustrated in Fig. 28. A T topology was selected for CM filter because the worst case CM noise impedance was calculated as 1.9 kΩ. The attenuation required was 57 at 0.6 MHz. A π topology was selected to suppress the DM noise, since this topology provides higher attenuation than other simple topologies such as the LC topology. The worst case DM noise impedance was 3 Ω. The required attenuation was 20 at 0.45 MHz. Finally, the components were selected and the combined EMI filter is displayed in Fig. 28. The test results for the filter are shown in Fig. 29. It is clear that the filter exceeded the FCC 15 Class B specifications across the entire frequency range by more than 3 dB.

The method presented is not only limited to single power supplies, but it can be used to design EMI filters for paralleled switching power supply modules. The paralleled power modules can be simplified to one equivalent power module, so the method presented can be used to design the EMI filter for a power system consisting of multiple power supplies.

VII. Conclusion

An improved method to design EMI filters was proposed. The method is based on measuring the noise spectrum and using the data to calculate the maximum possible value and minimum possible value of the noise impedance, and using it in the EMI filter design. The phase information of the noise impedance is not required when using the worst case, maximum or minimum possible value of the noise impedance. In addition, design procedures were outlined in sufficient detail so that the method could be implemented for future filter designs.

The proposed EMI filter design method successfully solved the limitations of the existing EMI filter design methods. Furthermore, it is useful for finding the right direction for EMI filter design work. The significant advantage of the new procedure is that it is easy to implement. Only the maximum and minimum amplitude of CM and DM noise source impedances are required. The designed filter will guarantee that the desired attenuation can be achieved. In addition, filters designed by the proposed method can meet the requirements in one design cycle.

Finally, EMI filters were designed for dc–dc and ac–dc SPSs. Experimental results were presented to demonstrate that this method is an effective and simple way to design EMI filters, while ensuring that the required attenuation can be achieved. In addition, this method can be used to design EMI filters for power systems with multiple power supplies.

REFERENCES

[1] F.-Y. Shih *et al.*, "A procedure for designing EMI filters for AC line applications," *IEEE Trans. Power Electron.*, vol. 11, pp. 170–181, Jan. 1996.

[2] D. Zhang, D. Y. Chen, M. J. Nave, and D. Sable, "Measurement of noise impedance of off-line converters," *IEEE Trans. Power Electron.*, vol. 15, pp. 820–825, Sept. 2000.

[3] T. Guo, D. Y. Chen, and F. C. Lee, "Separation of common-mode and differential-mode conducted EMI noise," *IEEE Trans. Power Electron.*, vol. 11, pp. 480–488, May 1996.

[4] *Input System Instability Application Note PQ-00-05-1 Rev. 01*, [Online] Available: http://www.synqor.com/support/3_1_app_notes.htm, 2004.

Sheng Ye (S'98) received the B.Sc. degree from the Department of Electrical Engineering, Hua Zhong University of Science and Technology, Wuhan, China, in 1998 and the M.Sc. degree from the Department of Electrical Engineering, Queen's University, Kingston, ON, Canada, in 2003 where he is currently pursuing the Ph.D. degree.

He was an R.D. Engineer in China from 1994 to 2001. His research fields are high efficiency dc–dc converters and EMI/EMC control in switching power supplies.

Wilson Eberle (S'98) was born in Windsor, ON, Canada. He received the B.Sc. and M.Sc. degrees from the Department of Electrical and Computer Engineering, Queen's University in Kingston, Kingston, ON, Canada, in 2000 and 2003, respectively, where he is currently pursuing the Ph.D. degree.

He was an Engineering Co-op Student with Ford Motor Company, Windsor, from 1997 to 1999. His research interests include high efficiency, high power density, low power dc–dc converters, digital control techniques for dc–dc converters, EMI filter design for switching converters, and large signal modeling of switching converters.

Mr. Eberle received the Ontario Graduate Scholarship.

Yan-Fei Liu (S'91–M'94–SM'97) received the B.Sc. and M.Sc. degrees from the Department of Electrical Engineering, Zhejiang University, Hangzhou, China, in 1984 and 1987, respectively, and the Ph.D. degree from the Department of Electrical and Computer Engineering, Queen's University, Kingston, ON, Canada, in 1994.

Since August 1999, he has been an Associate Professor with the Department of Electrical and Computer Engineering, Queen's University. From 1994 to 1999, he was a Technical Advisor with the Advanced Power System Division, Astec (formerly Nortel Networks), where he was responsible for high quality design, new products, and technology development. His research interests include digital control technologies for dc–dc switching converter and ac–dc converter with power factor correction, EMI filter design methodologies for switching converters, topologies and controls for high switching frequency, low switching loss converters, modeling and analysis of core loss and copper loss for high frequency planar magnetics, topologies and control for VRM, and large signal modeling of switching converters.

Dr. Liu received the Premiere's Research Excellent Award (PREA) in 2001, the Golden Apple Teaching Award in 2000, and the Award in Excellence in Technology from Nortel in 1997.